agronomy

MDPI

Article

A Promising, Highly Effective Nitrate Sorbent Derived from Solid Olive Mill Residues

José M. Angosto *, José M. Obón, María J. Roca, Mercedes Alacid and José A. Fernández-López

Department of Chemical and Environmental Engineering, Technical University of Cartagena (UPCT), Paseo Alfonso XIII, 52 E-30202 Cartagena, Spain; josemaria.obon@upct.es (J.M.O.); mariajo.roca@upct.es (M.J.R.); mercedes.alacid@upct.es (M.A.); josea.fernandez@upct.es (J.A.F.-L.)

* Correspondence: jm.angosto@upct.es; Tel.: +34-968327077

Abstract: Olive mill residues have been valorized by chemical modification with amines to improve their adsorption capacity and to be used as a low-cost bioadsorbent for nitrate removal. The Taguchi method was used to optimize the process. By performing a three-factor analysis with three levels, it was possible to significantly reduce the number of experiments to be performed and to obtain the best working conditions. The results of the Taguchi method showed that the highest adsorption capacity was 110 $mg \cdot g^{-1}$ with a functionalized biomass dose of 1 $g \cdot L^{-1}$ using an initial nitrate concentration of 500 $mg \cdot L^{-1}$. Field emission scanning electron microscopy (FESEM) and Fourier transform infrared spectroscopy (FTIR) were used to characterize the surface morphology and study the chemical changes that occurred in the biomass. For the best conditions of the Taguchi approach, the kinetic and equilibrium aspects of the adsorption process were analyzed. The adsorption isotherms obtained were successfully fitted to the Freundlich (R^2 = 0.98) and Langmuir (R^2 = 0.97) models. The kinetics of the process were studied, and the data obtained fit very well to the pseudo-second-order model (R^2 = 0.99). The adsorption values obtained suggest that it is a bioadsorbent with great potential for nitrate retention in aqueous solutions.

Keywords: nitrate adsorption; modified biomass; agrifood waste; Taguchi design; bioadsorption

Citation: Angosto, J.M.; Obón, J.M.; Roca, M.J.; Alacid, M.; Fernández-López, J.A. A Promising, Highly Effective Nitrate Sorbent Derived from Solid Olive Mill Residues. *Agronomy* **2023**, *13*, 1325. https://doi.org/10.3390/agronomy13051325

Academic Editor: Baskaran Stephen Inbaraj

Received: 13 April 2023
Revised: 3 May 2023
Accepted: 5 May 2023
Published: 9 May 2023

1. Introduction

Nowadays, of the most worrying environmental problems is the degradation of the quality of surface and groundwater, as determined by the environmental protection legislation of the most developed countries. Among the pollutants that have their origin in anthropogenic activity and are very frequently found in surface and groundwater bodies, the nitrate ion (NO^{3-}) stands out, which is a ubiquitous pollutant in the environment due to its high solubility and the difficulty for it to be fixed in the soil [1].

However, in high concentrations it has adverse effects on both humans and the environment, contributing to the eutrophication of aquatic environments and potentially increasing blood methemoglobin levels in humans (blue baby syndrome) [2]. The origin of this pollution lies mainly in poor agricultural practices, especially excessive nitrogen fertilization and the use of inappropriate forms of nitrogen, as well as inadequate management of livestock effluents [3]. Another cause of the increase in nitrate concentration is poor management of urban effluents.

Numerous methods have been employed for the removal of nitrates present in water, but none of them alone solve the problem. Nitrate removal technologies can be broadly divided into two categories: physico-chemical nitrate removal and biological nitrate reduction [4,5]. Physico-chemical methods are fairly well known and are based on membrane separation [6,7], ion exchange [8], chemical reduction [9–13] and adsorption [14–16]. Each of these technologies has its own strengths and drawbacks and their feasibility is weighed against factors such as application cost, disposal efficiency, the handling of waste generated and pre-treatment requirements [17].

In recent years, adsorption technology has been presented as an attractive method for the removal of contaminants present in aqueous effluents because it is fast, easy to apply, environmentally friendly and cost-effective [17–19]. To date, a large number of research and review papers have been published using different adsorbents used to remove contaminants from water [20–24].

The most commonly used commercial adsorbents to date are activated carbons, inorganic materials and ion exchange resins, but these materials have the disadvantages of a high cost, non-selectivity and difficulty of regeneration [19]. Hence, there is an interest in developing new adsorbents that overcome these drawbacks. In this sense, agri-food industry wastes are presented as materials with great potential to replace conventional adsorbents due to their low cost and high availability [19]. For the specific case of nitrate removal from aqueous solutions, carbon-based adsorbents, natural adsorbents, agricultural and industrial wastes and various other adsorbents have been used [25–27], although the main limitations of these by-products to remove pollutants from water are the low adsorption capacity and regeneration [19,28]. Hence, there is an interest in increasing their adsorption capacity by different techniques in order to increase the number of active sites.

Nitrate removal by adsorption is based on the interaction that occurs between the nitrate ion and the adsorbent, which transfers it from the aqueous solution to the adsorbent surface [2]. The aim of the adsorption process is to have an adsorbent with a high adsorption capacity and high selectivity for the nitrate ion, which can be achieved by modifying the structure of the adsorbent. Different methods have been used to modify the surface of adsorbents in order to improve nitrate retention capacity, including acid treatment (protonation), grafting of groups (carboxyl, hydroxyl or amine), metal or metal oxide impregnation and surfactant modification [2].

The selection of parameters, such as pH, initial nitrate concentration, adsorbent dosage, temperature and contact time, plays an important role in nitrate removal [2,29,30].

When it comes to studying the factors that affect one or more variables of interest, it is common to find situations in which the number of factors and the number of levels they can adopt is high. In these cases, carrying out a complete factorial design would involve a large investment of time and money. Therefore, to solve this problem, Taguchi proposed the use of orthogonal matrices, which make it possible to drastically reduce the number of experiments [31]. Moreover, after performing the experimental plan indicated by these matrices, the method also includes a statistical analysis of the results obtained, giving an answer to those optimal conditions, which reduces the variability of the process [32,33]. This method has been used to investigate the adsorption process for the removal of contaminants in water such as lead [33], cadmium [34], thorium [35], copper and nickel [36].

The first step in carrying out the Taguchi method is to identify the variable of interest, which in our case would be the nitrate adsorption capacity of the prepared adsorbent. Next, the factors that affect the adsorption capacity and the different levels they can present must be selected. Once the experimental results have been obtained, they are transformed into a measure of variability called signal-to-noise ratio (S/N). This represents the ratio between the mean (signal) and the standard deviation (noise). Therefore, the higher the S/N, the better the results, as there will be less variability [15].

To our knowledge, this is the first study on the use of chemically modified olive stone agri-food waste as an efficient and cost-effective adsorbent to remove nitrate ions present in aqueous solutions. Therefore, the main objective of this research is to apply Taguchi's design of experiments to identify the operational parameters that most influence nitrate bioadsorption in aqueous solutions when using lignocellulosic biomass from chemically modified olive stone agri-food waste as an adsorbent, in order to contribute to the circular economy. In fact, this study achieves a double benefit, on one hand valorizing this agri-food waste and, on the other hand, obtaining an improved and low-cost adsorbent with high affinity for nitrate ions. In addition, extensive isothermal and kinetic modeling studies have been carried out.

2. Materials and Methods

2.1. Preparation, Chemical Modification and Characterization of the Sorbent

Agro-food waste biomass from olive oil mills in the Region of Murcia, a typical area of this crop in south-eastern Spain, was used. The starting materials, olive mill residues (OMR), were washed with distilled water and dried at 70 °C for 24 h before being ground and passed through a sieve to obtain three powder fractions (0.2–0.5 mm, 0.5–0.8 mm and 0.8–1 mm) for use.

The prepared OMR fractions were subjected to chemical modification [37], with some modifications to the temperatures used (Figure 1). Twenty grams of each of the particle size fractions were taken and placed separately into 250 mL Erlenmeyer flasks. For each flask, 20 mL of epichlorohydrin and 18 mL of N,N-dimethylformamide were first added and shaken for 1 h at 95 °C. Secondly, 6 mL of diethylenetriamine was added and stirred for 1 h at 95 °C. Thirdly, 18 mL of triethylamine was added and stirred for 1 h at 95 °C. The product from each flask was washed with distilled water, filtered, dried for 24 h at 100 °C and stored in a desiccator for use in adsorption experiments (MOMR).

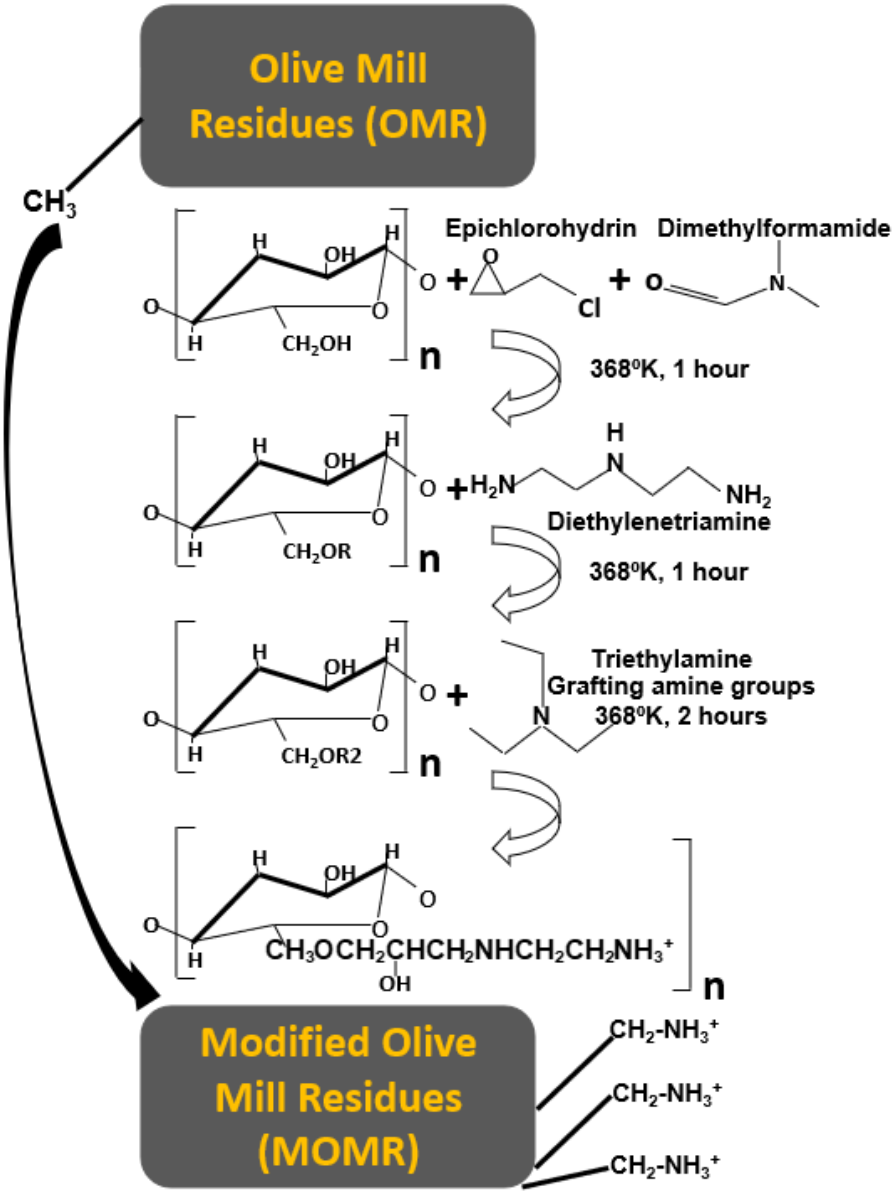

Figure 1. Mechanism of biomass activation by grafting of amino groups.

Surface characterization of the adsorbents before modification (OMR), after chemical modification (MOMR) and after nitrate retention (MOMR-N) was performed by field emission scanning electron microscopy (FESEM) and Fourier transform infrared spectroscopy (FTIR).

A ZeissCrossbeam 350 field emission scanning electron microscope (FESEM) (Carl Zeiss Microscopy GmbH, Oberkochen, Germany) was used to analyze the morphology of the prepared materials at different magnifications. The SEM observation conditions were an accelerating voltage of 10 kV and a working distance in the order of 5 mm. The image was generated with the secondary electron signal (SE Secondary Electron) under variable pressure conditions (30 Pa). A Zeiss SmartSEM operating system version 6.07 (2020) was used for image acquisition. In addition, X-ray energy dispersive (EDX) microanalyses and surface mapping were performed using an Oxford Instrument UK EDX detector and AZtec software version 5.0.7577.2 (2020).

Using Fourier transform infrared spectroscopy (FITIR), room temperature infrared spectra were obtained to identify the functional groups present on the surface of the different sorbents. A Thermo Nicolet 5700 (ThermoFisher Scientific, Karlsruhe, Germany) was used in the range of 4000 to 500 cm^{-1} and in transmittance mode.

2.2. Experimental Design Using Taguchi

The nitrate adsorption capacity of the prepared adsorbent was selected as the variable of interest to identify the best experimental conditions with the least variability. The next step was to select factors that affect the adsorption capacity that we can control in our experimental assays. Three controllable factors (sorbent dosage, initial nitrate concentration and sorbent particle size) were considered at three levels (Table 1). To carry out the Taguchi method, Minitab 19 statistical software was used and an L9 orthogonal matrix was obtained, with nine different experiments that were initially carried out.

Table 1. Controllable factors and their levels.

Factor	Description	Level 1	Level 2	Level 3
A	Sorbent dosage ($g \cdot L^{-1}$)	0.5	1.0	2.0
B	Initial nitrate concentration ($mg \cdot L^{-1}$)	40	200	400
C	Sorbent particle size (mm)	0.2–0.5	0.5–0.8	0.8–1.0

According to the Taguchi approach, once the adsorption capacity values are obtained, they are transformed to a measure of variability called the signal-to-noise ratio (S/N) [15]. The S/N ratio is analyzed to evaluate the experimental results. There are three ways to calculate the S/N, and the choice of one or the others depends on the variable of interest to be optimized: (1) smaller is better, (2) nominal is better and (3) larger is better [29]. In this case, as the adsorption capacity is the variable of interest and we wish for it to be as high as possible; thus, the S/N rate is taken is the largest is the best, which is calculated by Equation (1) [23]:

$$S/N = -10 \log_{10}\left[\frac{1}{n}\sum_{i=1}^{n}\left(\frac{1}{y_i}\right)^2\right] \quad (1)$$

where n is the number of replicates of each trial and y represents the sorption capacity obtained in experiment i. An analysis of variance (ANOVA) was used to determine the effect of factors on sorption capacities [38]. Minitab 19 software was used in the Taguchi approach.

2.3. Sorption Tests

A nitrate stock solution (1000 $mg \cdot L^{-1}$) was prepared by dissolving KNO_3 in Milli Q water. The stock solution was diluted with Milli Q water to a certain nitrate concentration prior to the experiments. The pH was adjusted to pH 7 using NaOH and/or HCl solutions (0.1 M). Batch sorption experiments were carried out by stirring 100 mL of nitrate solution at a fixed concentration (C_0) and a known amount of sorbent on an orbital shaker (150 rpm, 24 h) at room temperature. The solutions were then filtered and the residual nitrate

concentration in the solution was quantified (C_e). Analytical determinations of C_0 and C_e were carried out using a compact UV/VIS ion chromatograph (Agilent 1290 Infinity II LC, Agilent >Technologies, Santa Clara, CA, USA).

The amounts of nitrate adsorbed at equilibrium (q_e), evaluated as mg nitrate/g biomass used, were determined by the mass balance equation (Equation (2)) from the values of nitrate concentration in the solution at the beginning (C_0) and at the end of the test (C_e):

$$q_e\ (\mathrm{mg}\cdot\mathrm{g}^{-1}) = \frac{(C_0 - C_e)\cdot V}{m} \quad (2)$$

where V is the solution volume (L) and m is the sorbent dry weight (g).

2.3.1. Adsorption Isotherm Study

It is of great interest to study the equilibrium data in order to fit different theoretical models that allow a quantitative description of the adsorption processes.

For the study of the adsorption isotherms, the best conditions obtained according to Taguchi's method were used (sorbent dose: 1 $g\cdot L^{-1}$ and fraction: 0.2–0.5 mm). Regarding the initial nitrate concentration, six solutions were prepared with different concentrations in the range of 40–400 $mg\cdot L^{-1}$ of KNO_3 and adjusting the pH to 7. The suspension obtained in each case was placed in an orbital shaker and maintained at 150 rpm and room temperature for 24 h. The experimental data obtained were adjusted to the desired concentration. Sample treatment and determination were carried out as described in Section 2.3.

The experimental data obtained were adjusted to the Langmuir and Freundlich equations to model the adsorption isotherms and better understand the adsorption process [33,39].

2.3.2. Adsorption Kinetics Study

For kinetic experiments, 1 g of adsorbent (MOMR of particle size 0.2–0.5 mm) was mixed with 1000 mL of KNO_3 solution of 400 $mg\cdot L^{-1}$. It was kept at room temperature with constant stirring for 24 h (150 rpm). Samples were taken at the required intervals. Treatment and determination of nitrate concentrations were carried out as described in Section 2.3.

3. Results and Discussion

3.1. Optimization of the Taguchi Experiments

Table 2 shows the nitrate removal efficiencies (q_e) in each of the experiments performed according to the Taguchi design. Each test condition was repeated three times. It can be seen that the highest sorption efficiency for nitrate ions occurred in experiment 6 (110 $mg\cdot g^{-1}$). We note that the removal efficiency is strongly influenced by the parametric conditions employed.

Table 2. L9 orthogonal array for each of the experiments performed and results obtained for nitrate removal efficiency (q_e) and signal-to-noise (S/N) ratio (mean ± D; n = 3).

RUN	Sorbent Dosage ($g\cdot L^{-1}$)	$[NO_3^-]$ ($g\cdot L^{-1}$)	Particle Size (mm)	q_e ($mg\cdot g^{-1}$)	*S/N* Ratio
1	0.5	40	0.2–0.5	34 ± 0.2	30.63 ± 0.3
2	0.5	200	0.5–0.8	40 ± 0.3	32.04 ± 0.2
3	0.5	400	0.8–1.0	40 ± 0.2	32.04 ± 0.2
4	1.0	40	0.5–0.8	24 ± 0.4	27.60 ± 0.2
5	1.0	200	0.8–1.0	60 ± 0.3	35.56 ± 0.3
6	1.0	400	0.2–0.5	110 ± 0.5	40.83 ± 0.4
7	2.0	40	0.8–0.1	13.5 ± 0.2	22.61 ± 0.2
8	2.0	200	0.2–0.5	57.5 ± 0.4	35.19 ± 0.3
9	2.0	400	0.5–0.8	45 ± 0.3	33.06 ± 0.3

The S/N ratio for each factor at levels 1, 2 and 3, together with the total increments (delta values) and ranges, are given in Table 3. In Table 3, in relation to the levels stage, with the S/N as the desired response characteristic, the particle size employed showed the greatest influence at level 1. At level 2, the adsorbent dose followed by the initial nitrate concentration showed the greatest influence, with very similar values. At level 3, it was the nitrate concentration that showed the greatest influence. The delta value, which represents the relative influence of each effect [40], shows that it is the initial nitrate concentration that most affected the S/N ratio.

Table 3. Average of the response characteristic at each level of the signal-to-noise ratio (S/N) factor (bigger is better).

Level	Sorbent Dosage	$[NO_3^-]$ $(g \cdot L^{-1})$	Particle Size
L1	31.5	26.9	35.5
L2	34.6	34.2	30.9
L3	30.2	35.3	30.1
Delta	4.3	8.36	5.48
Rank	3	1	2

In order to easily visualize the variation of the response with the change in the levels of a parameter, the response curves are presented in Figure 2. The individual effects of the nitrate adsorption parameters on the sorption capacities (q_e) and the respective S/N ratios can be studied, and the general trend of the influence of the three factors considered can be quickly appreciated.

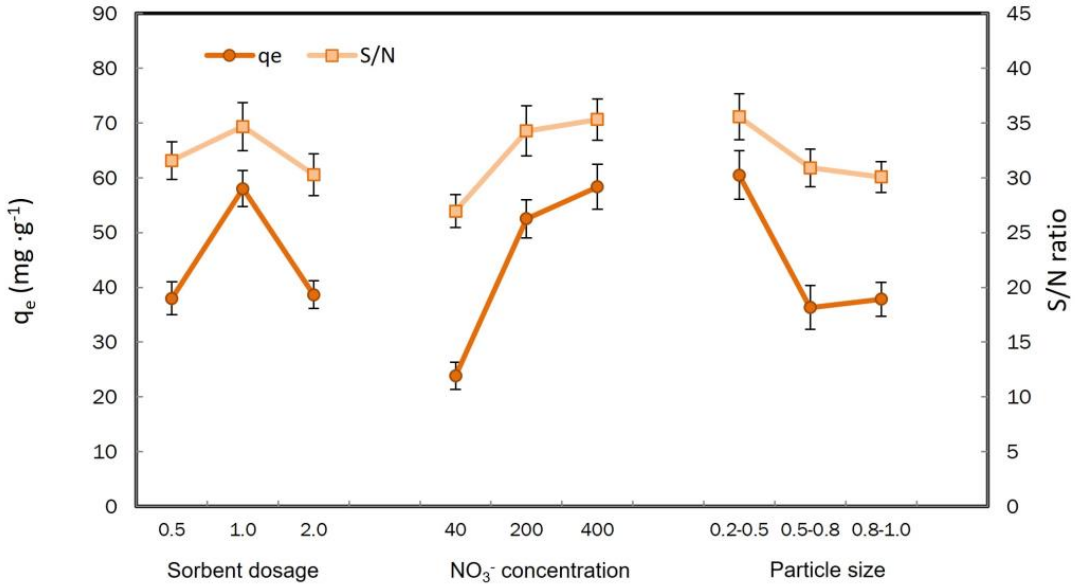

Figure 2. Effect of factors on q_e and the S/N ratio for nitrate adsorption.

The adsorbent dose has an important influence on the adsorption process. On the one hand, the surface area and the number of active sites increases with adsorbent dose, so nitrate adsorption should increase with increasing adsorbent dose [41], but on the other hand, overlapping adsorption sites may decrease the total surface area, thus decreasing the adsorption capacity with an increasing adsorbent dose [42]. The effect of the adsorbent dose on the S/N ratio and the q_e value indicated an increase in the response curve as the dose increased from 0.5 to 1 $g \cdot L^{-1}$ and a decrease when the adsorbent dose was increased to 2 $g \cdot L^{-1}$. The maximum adsorption, according to the response curve in Figure 2, was reached for an adsorbent dose of 1.0 $g \cdot L^{-1}$.

Nitrate adsorption was significantly affected by the starting concentration, as the arrival of nitrate ions at the adsorbent surface is influenced by the initial nitrate concentration [41]. The S/N ratio of nitrate adsorption increased as the starting concentration increased from 50 to 500 mg·L^{-1}.

The particle size of the adsorbent also has a great influence on the adsorption capacity of nitrate ions, as shown in Figure 3. It is observed that the maximum adsorption capacity and the highest S/N value is obtained for the fraction between 0.2 and 0.5 mm, since for this smaller size there is an increase in active sites that would facilitate the adsorption of nitrate ions [42].

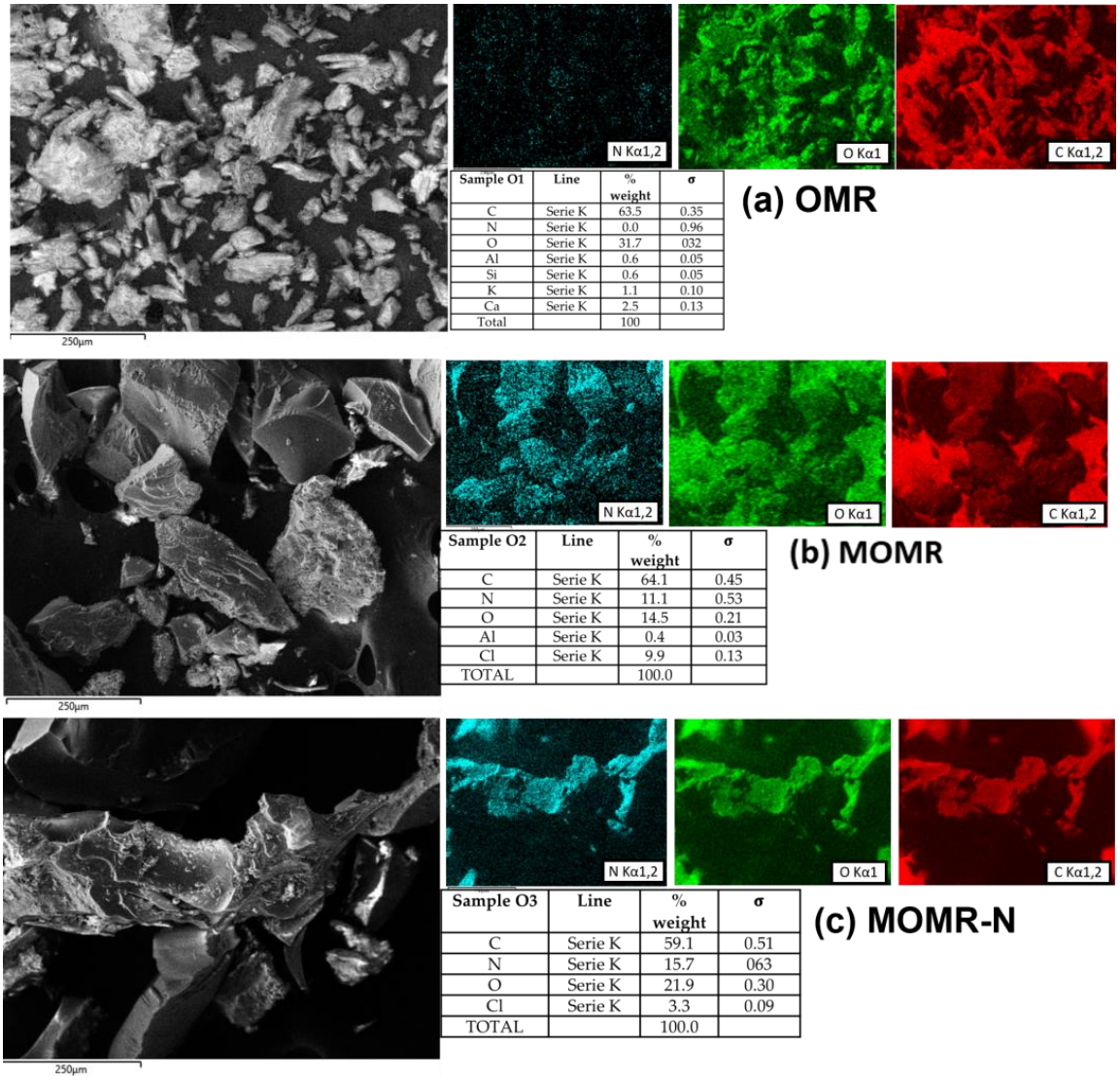

Sample O1	Line	% weight	σ
C	Serie K	63.5	0.35
N	Serie K	0.0	0.96
O	Serie K	31.7	032
Al	Serie K	0.6	0.05
Si	Serie K	0.6	0.05
K	Serie K	1.1	0.10
Ca	Serie K	2.5	0.13
Total		100	

Sample O2	Line	% weight	σ
C	Serie K	64.1	0.45
N	Serie K	11.1	0.53
O	Serie K	14.5	0.21
Al	Serie K	0.4	0.03
Cl	Serie K	9.9	0.13
TOTAL		100.0	

Sample O3	Line	% weight	σ
C	Serie K	59.1	0.51
N	Serie K	15.7	063
O	Serie K	21.9	0.30
Cl	Serie K	3.3	0.09
TOTAL		100.0	

Figure 3. FESEM micrographs of biomasses: (**a**) raw biomass before modification (OMR), (**b**) after chemical modification (MOMR) and (**c**) after nitrate adsorption (MOMR-N).

Therefore, after analyzing the results of the Taguchi analysis, we can affirm that a nitrate concentration of 500 ppm, a particle size of 0.2–0.5 mm and an adsorbent dose of 1 g·L^{-1} allowed obtaining the highest nitrate adsorption, so they were chosen as the best conditions. From the ANOVA results, we can confirm that the initial nitrate concentration has a contribution of 60.11% in the adsorption process; the adsorbent fraction contributes 25.23% and the adsorbent dose contributes 14.65%.

3.2. Biomass Characterization

Field Emission Scanning Electron Microscopy (FESEM)

In Figure 3, FESEM micrographs of the crude biomass before modification (OMR), after chemical modification (MOMR) and after nitrate adsorption (MOMR-N) are presented for the particle fraction between 0.2 and 0.5 mm.

Field emission scanning electron microscopy with an EDS instrument (FESEM-EDS) is a very powerful and widely used tool for analysis of the surface morphology of materials prepared at different magnifications and for the determination of elemental compositions [43,44].

The micrographs presented in Figure 3a–c, illustrate in general a typical surface structure of a lignocellulosic biomass [45], characterized by a consistent, firm structure; the presence of cavities; irregular dimensions; and a slightly porous nature due to the predominance of olive pits. There is a greater predominance of irregular shapes and heterogeneous surfaces for the case of OMR before chemical modification (Figure 3a). In the modified biomass (MOMR) (Figure 3b) and in the nitrate-loaded biomass (MOMR-N) (Figure 3c), there is an increase in particle size due to the surface coating of the biomass functionalization, a decrease in these irregular shapes, a lower presence of pores and a higher consistency than in OMR (Figure 3a).

The elemental chemical composition of the crude biomass (OMR) is illustrated in Figure 3a, which shows that, as expected, C and O are the predominant elements [46], while other elements such as Al, Si, K and Ca were also detected at the surface, but in very low amounts. When the chemical modification (MOMR) is performed, as shown in Figure 3b, there is a change in the elemental composition; the N and Cl content increases significantly as a consequence of the reagents used in the functionalization. Finally, Figure 3c shows that for the charged biomass, which has been in contact with nitrates (MOMR-N), there is still a significant increase in the N content, which allows us to demonstrate the efficiency of the charged biomass to retain nitrate ions.

3.3. Fourier Transform Infrared Spectroscopy (FTIR)

Fourier transform infrared spectroscopy (FTIR) is a very valuable technique to perform qualitative analyses of the main functional groups involved in the binding of nitrates to the bioadsorbent employed [33]. Figure 4 shows the FTIR spectra in the finger region (4000–500 cm^{-1}) of the different biomasses employed in this study (OMR, MOMR and MOMR-N).

For all samples, a broad band is observed around 3200 cm^{-1}, which shifts to the right for the modified (MOMR) and nitrate-loaded (MOMR-N) biomasses, which could indicate the presence of -OH and -NH groups. Another region where important changes occur is in the band between 2800 cm^{-1} and 2900 cm^{-1}. In this region, the spectra obtained for the chemically modified biomass (MOMR) and the loaded biomass (MOMR-N) differ significantly from that of the raw biomass (OMR). These changes may be due, respectively, to the asymmetric stretching vibration of the -CH_2 and symmetric stretching of the -CH_3 group present in the aliphatic acids [47]. A band was recorded around 1650 cm^{-1}, which is characteristic of the stretching vibrations of carboxyl groups [45–48].

The most significant changes are seen in the region from 1200 to 1500 cm^{-1}, which allows us to affirm that the functionalities of lignin and amino groups intervened in the bioadsorption process, being observed to a greater extent for the loaded biomass (MOMR-N). The band at 1300 cm^{-1} may indicate the stretching of the C-N bond [49]. This could be due to asymmetric stretching of nitrate anions retained by the biomass [50].

Therefore, when comparing the FITIR spectra of the three biomasses used in the study, significant changes in the structure of the peaks obtained can be seen, both in their position and intensity, which confirms the participation of the groups associated with these bands in the process of biomass functionalization and nitrate bioadsorption.

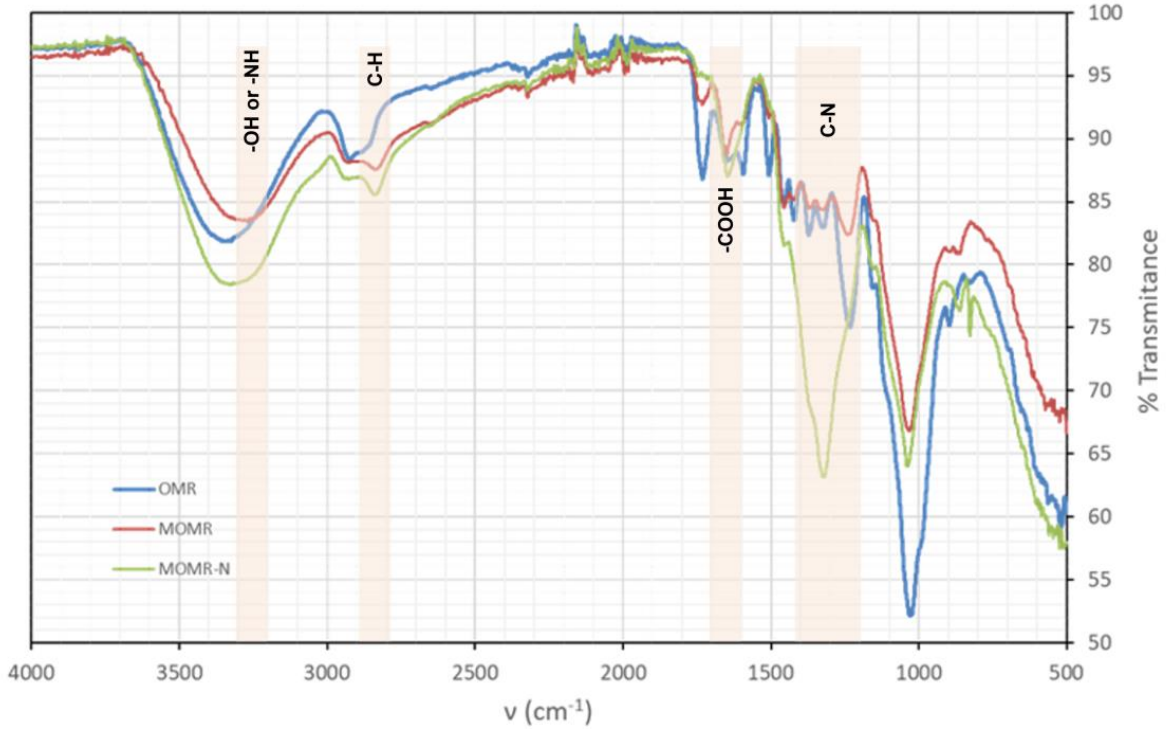

Figure 4. FTIR spectra of raw biomass (OMR), modified biomass (MOMR) and modified and nitrate-loaded biomass (MOMR-N).

3.4. Sorption Isotherms

Adsorption isotherms are very useful to obtain information about the interaction between the adsorbate and the adsorbent [2,51], as well as to determine the adsorption capacity and mechanism [52]. The isotherms describe the interaction between the two phases that compose the adsorption system, the nitrate ions and the functionalized biomass (MOMR). There is no single isotherm equation that correctly fits all the experimental data. However, the goal of this study is to find an isotherm model that fits the experimental data as well as possible in order to advance the design of adsorption systems.

The experiments were performed following the optimal operating conditions suggested by the Taguchi approach. From the equilibrium data, the adsorption process was studied by fitting the experimental data to the most commonly used mathematical models [53], presenting the results of the Langmuir and Freundlich models, which provided the best fit, and which correspond to homogeneous and heterogeneous adsorption surfaces, respectively [53]. Moreover, they are the most commonly used adsorption isotherms to study the adsorption of contaminants in the liquid phase [54,55].

Figure 5 shows the fit of the experimental data to the Langmuir and Freundlich isotherm models, respectively. Although the fit is very similar in a both cases, the fit is slightly better for the Freundlich model, with an R^2 of 0.98 versus an R^2 of 0.97 for the Langmuir model.

Table 4 presents the values of the relative constants of the models used. The Langmuir constant (K_L) provides information on the affinity of the modified biomass for nitrate ions. The value obtained (K_L = 0.0153 mg·L^{-1}), well below one, suggests that the binding forces are strong, which could indicate the presence of chemisorption [56]. This adsorption model, which assumes monolayer adsorption, considers that it is homogeneous and occurs on identical and equivalently defined active sites [57], compatible with chemically modified biomass.

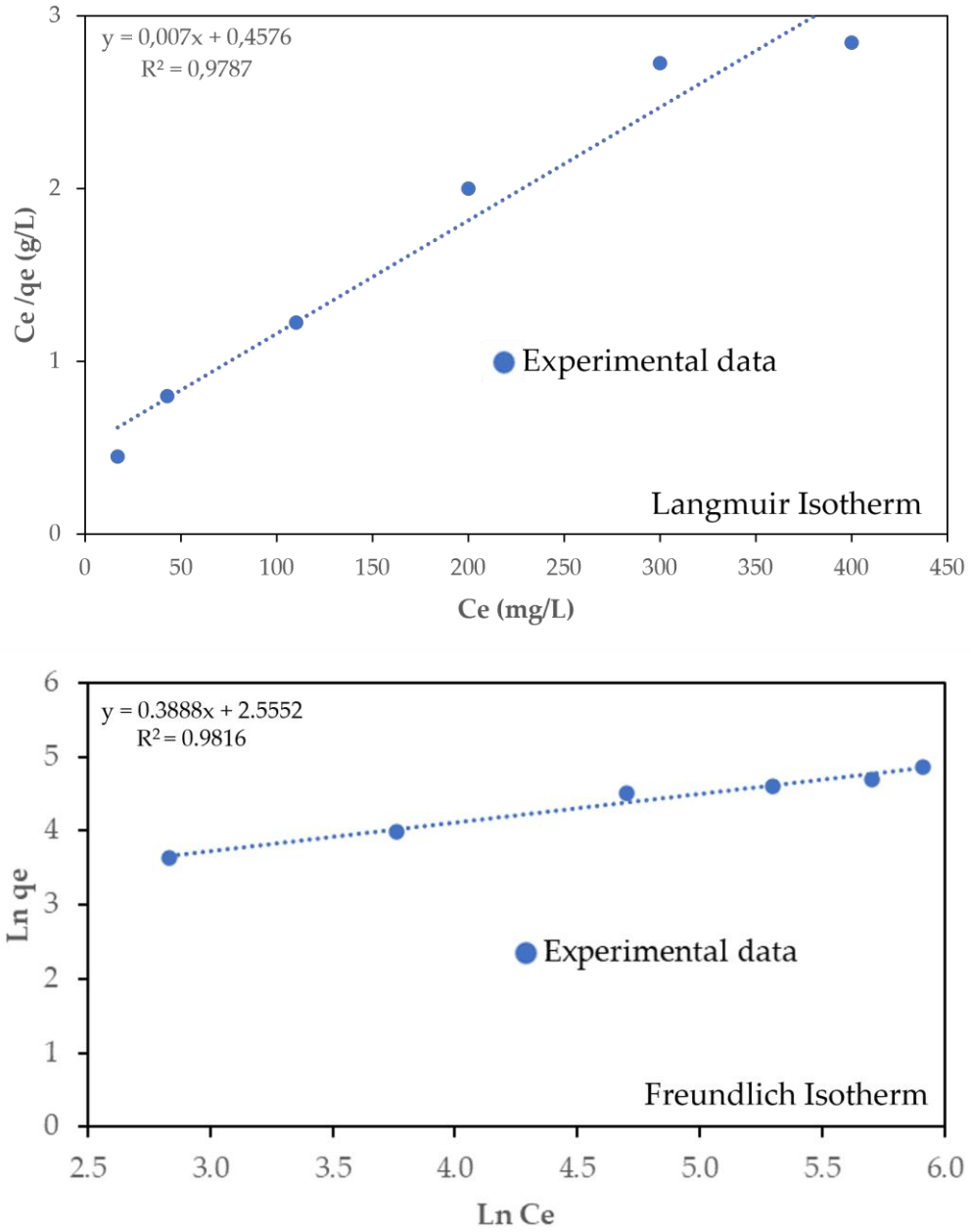

Figure 5. Langmuir and Freundlich isotherms.

Table 4. Isotherm Langmuir and Freundlich parameters.

Langmuir			Freundlich		
q_{max} (mg·g^{-1})	k_L (mg·L^{-1})	R^2	K_F (mg·g^{-1})	n	R^2
142.86	0.0153	0.979	12.86	2.57	0.982

In addition, the K_L value was used to calculate the dimensionless factor (R_L), which provides information on the affinity of the biomass used for nitrate ions [58]. The R_L value is obtained from the following equation (Equation (3)):

$$R_L = \frac{1}{1 + K_L \cdot C_0} \quad (3)$$

where C_0 is the initial nitrate concentration. Values between 0 and 1 suggest that this is a thermodynamically favorable process. For the initial nitrate concentrations used, R_L values of less than one (between 0.79 and 0.15) were obtained in all cases, indicating that nitrate adsorption with this modified biomass is a favorable process, and as the initial nitrate concentration increases, the process becomes more favorable. The maximum nitrate adsorption capacity estimated by the Langmuir model was 142.86 $mg \cdot g^{-1}$, a value higher than those obtained in the Taguchi experiments (Table 2).

The Freundlich isotherm is an empirical model describing non-ideal and reversible adsorption, that can be monolayer or multilayer, with a non-uniform distribution of affinities over the heterogeneous surface and also non-uniform distribution [53,55]. As seen in Figure 4 and Table 4, the experimental data fit quite well, with a correlation coefficient of 0.98. The Freundlich coefficient, K_F, describes the adsorption capacity. The slope 1/n, derived from the equation in Figure 4, can be interpreted as a measure of the adsorption intensity [59], and when it is below zero, it is considered to be a chemisorption process. The correlation coefficients (R^2) obtained show the compatibility of the Langmuir and Freundlich isotherms to explain the sorption of nitrate ions in monolayers on the modified biomass. The fit in both cases is very similar.

3.5. Sorption Kinetics

A kinetic study is important for understanding the adsorption process, as it allows distinguishing the reaction pathways and mechanisms and the stages that control the rate, as well as obtaining valuable information about the possible mechanisms that control the adsorption process [60].

In addition, it allows predicting the transfer rate of nitrate ions on the surface of the modified biomass, which is essential for selecting and designing large-scale batch processes, as it helps us to define the retention time necessary to carry out a continuous adsorption process, and therefore it will determine the efficiency of the system [61].

A kinetic study was developed for the optimum conditions defined by Taguchi's method, i.e., with a chemically modified biomass dose of 1 g/L, an adsorbent particle size of 0.2–0.5 mm and starting from a nitrate solution of 500 mg/L.

Figure 6 shows the effect of time on NO^{3-} sorption by the chemically modified biomass (MOMR-N). It is observed that the sorption of nitrate ions increased very rapidly at the beginning. Only 6 min after the beginning of the experiment, 72.72% of the concentration reached at equilibrium was adsorbed, which gives us an idea of the great power of the biomass activated with amines in adsorption processes.

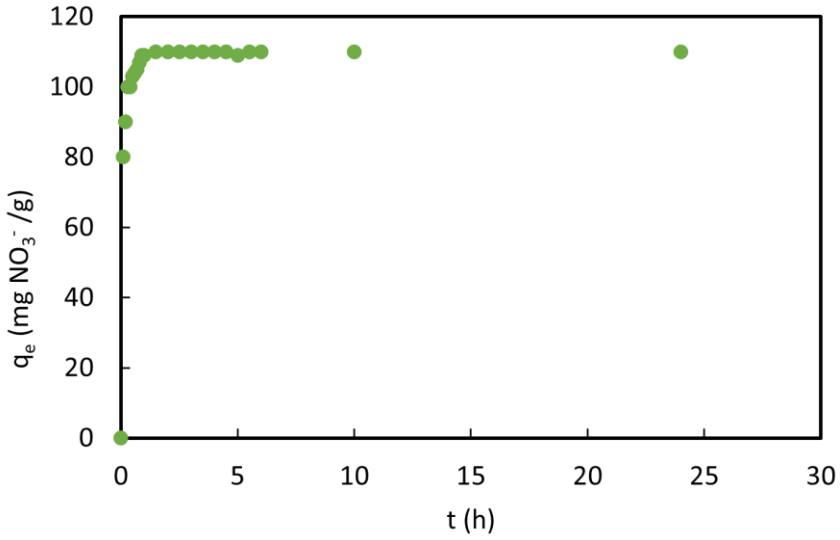

Figure 6. Kinetics of nitrate adsorption by chemically modified biomass (MOMR).

In order to better understand the adsorption process, the nitrate adsorption kinetics were determined by mathematically fitting the data obtained in the kinetic study to the adsorption–reaction kinetic models and pseudo-first-order and pseudo-second-order kinetic models.

The parameters and kinetic coefficients of the models used are shown in Table 5. It was the pseudo-second-order model that presented a better coefficient of determination (R^2 = 0.99) compared to the pseudo-first-order model which presented a coefficient of determination R^2 of 0.93. These parameters confirm that the model that best describes the adsorption process of nitrate ions on chemically modified biomass is the pseudo-second-order model. Moreover, the calculated value for the adsorption capacity (q_e) corresponds very well with the experimentally measured value. As it fits very well to pseudo-second-order kinetics, it allows us to affirm that this is a chemisorption process [54].

Table 5. Model kinetic parameters.

Nitrate Ion	Pseudo-First-Order			Pseudo-Second-Order		
	q_e (mg·g^{-1})	k_1 (h^{-1})	R^2	q_e (mg·g^{-1})	k_2 (g·mg^{-1}·h^{-1})	R^2
NO^{3-}	57.12	1.76	0.93	110.16	0.41	0.99

As for the adsorption mechanism (Figure 7), we can state that it takes place in different steps. First, the nitrate ions create a film around the adsorbent. Secondly, nitrate ions diffuse on the external surface, and finally, adsorption takes place on the surface of the adsorbent modified with amino groups.

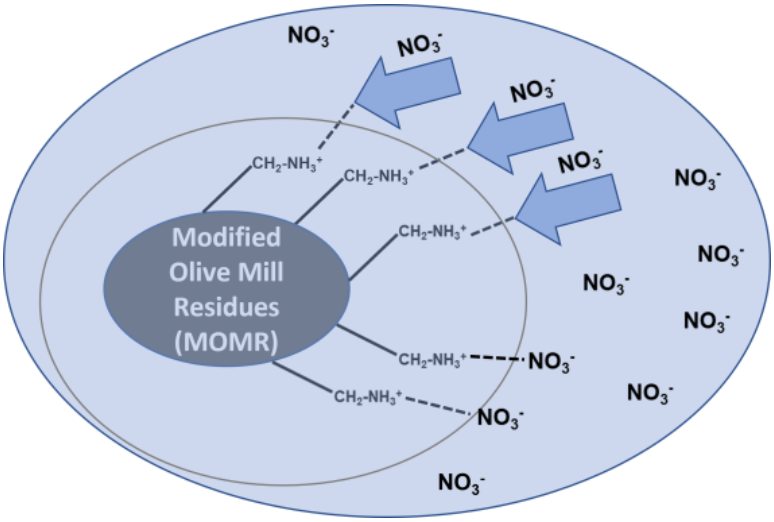

Figure 7. Proposed mechanism of nitrate ion adsorption on MOMR.

Comparing the nitrate removal values obtained in this work (MOMR-N) with those of other modified bioadsorbents reported in the literature (Table 6), we can affirm that in this study we achieved intermediate nitrate removal values (110 mg·g^{-1}). We have no data on the use of this modified biomass for nitrate removal in aqueous solutions. The retention capacity finally achieved is influenced by the composition of the biomass used and by the method employed for chemical modification. In our case, the chemical modification carried out allows us to valorize a very low-cost and widely available agri-food waste, as well as to achieve a nitrate ion retention capacity such that the process may be potentially used in a column.

Table 6. Nitrate adsorption capacities of modified biomasses.

Bioadsorbent	Adsorption Capacity ($mg \cdot g^{-1}$)	Reference
Modified steel slag	16.40	[62]
Modified cocoa shell	31.65	[63]
Modified cocoa shell	56.95	[54]
Amine cross-linked reed	102.00	[64]
Amine cross-linked tea wastes	136.43	[65]
Modified pine sawdust	145.26	[66]
Modified olive mill residues	110.00	Present study

4. Conclusions

This study has shown that the valorization of olive mill residues chemically modified with amines significantly improves their adsorption capacity with respect to the crude biomass, and that it is effective for the removal of nitrates from aqueous solutions. The Taguchi factorial design allowed optimizing the operating conditions (adsorbent dose: 1 $g \cdot L^{-1}$; nitrate concentration: 500 $mg \cdot L^{-1}$ and adsorbent size: 0.2–0.5 mm). Biomass characterization by FESEM and FTIR revealed significant changes in both the chemically modified and nitrate-loaded biomass. Under the optimum conditions of the Taguchi approach, a nitrate adsorption capacity of 110 $mg \cdot g^{-1}$ was experimentally obtained. The Freundlich model presented the best correlation with nitrate removal, showing that the modified adsorbent has a good and strong adsorption capacity. The pseudo-second-order kinetic model best explained the kinetics of the process, with the chemisorption process predominating. The experimental results obtained suggest that this is an adsorbent with a high potential for nitrate removal in aqueous solutions, so it would be interesting to test its behavior in continuous studies.

Author Contributions: Conceptualization, J.M.A. and J.A.F.-L.; methodology, J.M.A. and J.M.O.; investigation, J.M.A., M.A., M.J.R. and J.M.O.; data curation, J.M.A., J.A.F.-L. and J.M.O.; writing—original draft preparation, J.M.A. and J.A.F.-L.; writing—review and editing, J.M.A., J.A.F.-L., J.M.O., M.A. and M.J.R.; funding acquisition, J.M.A. All authors have read and agreed to the published version of the manuscript.

Funding: This research was funded by the Project 2I20SAE00081 through the Call for Public Grants to finance the strategic projects included in the Research and Innovation Strategy for Smart Specialisation-RIS3MUR Strategy by the Autonomous Community of the Region of Murcia (CARM), Spain, within the framework of the FEDER Operational Program Region of Murcia 2014–2020 under the thematic objective 1: Strengthen research, technological development and innovation by 80% and with CARMs own funds by 20%.

Data Availability Statement: Not applicable.

Conflicts of Interest: The authors declare no conflict of interest.

References

1. Abascal, E.; Gómez-Coma, I.; Ortiz, I.; Ortiz, A. Global dignosis of nitrate pollution in groundwater and review of removal technologies. *Sci. Total Environ.* **2022**, *810*, 152233. [CrossRef] [PubMed]
2. Liu, Y.; Zhang, X.; Wang, J. A critical review of various adsorbents for selective removal of nitrate from water: Structure, performance and mechanism. *Chemosphere* **2022**, *291*, 132728. [CrossRef]
3. Tokazhanov, G.; Ramazanova, E.; Hamid, S.; Bae, S.; Lee, W. Advances in catalytic reduction of nitrate by metallic catalysts for high efficiency and N_2 selectivity: A review. *Chem. Eng. J.* **2020**, *384*, 123252. [CrossRef]
4. Weilgelhofer, G.; Hein, T. Efficiency and detrimental side effects of denitrifying bioreactors for nitrate reduction in drainage water. *Environ. Sci. Pollut. Res.* **2015**, *22*, 13534–13545. [CrossRef] [PubMed]
5. Pang, Y.; Wang, J. Various electron donors for biological nitrate removal: A review. *Sci. Total Environ.* **2021**, *794*, 148699. [CrossRef] [PubMed]
6. Giwa, A.; Dufour, V.; Al Marzooqi, F.; Al Kaabi, M.; Hasan, S.W. Brine management methods: Recent innovations and current status. *Desalination* **2017**, *407*, 1–23. [CrossRef]

7. Wang, J.; Liu, X. Forward osmosis technology for water treatment: Recent advances and future perspectives. *J. Clean. Prod.* **2021**, *280*, 124354. [CrossRef]
8. Palko, J.W.; Oyarzun, D.I.; Ha, B.; Stadermann, M.; Santiago, J.G. Nitrate removal from water using electrostatic regeneration of functionalized adsorbent. *Chem. Eng. J.* **2018**, *334*, 1289–1296. [CrossRef]
9. Fanning, J.C. The chemical reduction of nitrate in aqueous solution. *Coord. Chem. Rev.* **2000**, *199*, 159–179. [CrossRef]
10. Wang, J.; Chu, L. Biological nitrate removal from water and wastewater by solid-phase denitrification process. *Biothechn. Adv.* **2016**, *34*, 1103–1112. [CrossRef]
11. Xu, J.; Pu, Y.; Qi, W.; Yang, X.J.; Tang, Y.; Wan, P.; Fisher, A. Chemical removal of nitrate from water by aluminum-iron alloys. *Chemosphere* **2017**, *166*, 197–202. [CrossRef] [PubMed]
12. Wang, J.L.; Guo, X. Adsorption isotherm models: Classification, physical meaning, application and solving method. *Chemosphere* **2020**, *258*, 127279. [CrossRef] [PubMed]
13. An, B.; He, H.; Duan, B.; Deng, J.; Liu, Y. Selective reduction of nitrite to nitrogen gas by CO2 anion radical from the activation of oxalate. *Chemosphere* **2021**, *278*, 130388. [CrossRef] [PubMed]
14. Wang, J.L.; Zhuang, S.T. Removal of various pollutants from water and wastewaters by modified chitosan adsorbents. *Crit. Rev. Environ. Sci. Technol.* **2017**, *47*, 2331–2386. [CrossRef]
15. Rosique, M.; Angosto, J.M.; Guibal, E.; Roca, M.J.; Fernández-López, J.A. Factorial design methodological approach for enhanced cadmium ions bioremoval by Opuntia biomass. *CLEAN Soil Air Water* **2016**, *44*, 959–966. [CrossRef]
16. Saavedra, M.I.; Doval Miñarro, M.; Angosto, J.M.; Fernández-López, J.A. Reuse potential of residues of artichoke (*Cynara scolymus* L.) from industrial canning processing as sorbent of heavy metals in multimetallic effluents. *Ind. Crops Prod.* **2019**, *141*, 111751. [CrossRef]
17. Singh, N.B.; Nagpal, G.; Rachna, S.A. Water purification by using adsorbents: A review. *Environ. Technol. Innov.* **2018**, *11*, 187–240. [CrossRef]
18. Dovi, E.; Kani, A.N.; Aryee, A.A.; Jie, M.; Li, J.J.; Li, Z.H.; Qu, L.B.; Han, R.P. Decontamination of bisphenol A and congo red dye from solution by using CTAB functionalized walnut shell. *Environ. Sci. Pollut. Res.* **2021**, *28*, 28732–28749. [CrossRef]
19. Kani, A.N.; Dovi, E.; Mptani, F.M.; Aryee, A.A.; Han, R.; Li, Z.; Qu, L. Pollutant decontamination by polyethyleneimineengineered agricultural waste materials: A review. *Environ. Chem. Lett.* **2022**, *20*, 705–729. [CrossRef]
20. Fernández-López, J.A.; Angosto, J.M.; Avilés, M.D. Biosorption of hexavalent chromium from aqueous medium with *Opuntia biomass*. *Sci. World J.* **2014**, *2014*, 670249. [CrossRef]
21. Raval, N.P.; Shah, P.U.; Shah, N.K. Adsorptive removal of nickel (II) ions from aqueous environment: A review. *J. Environ. Manag.* **2016**, *179*, 1–20. [CrossRef] [PubMed]
22. Zhuang, S.; Liu, Y.; Wang, J.L. Mechanistic insight into the adsorption of diclofenac by MIL-100: Experiments and theoretical calculations. *Environ. Pollut.* **2019**, *253*, 616–624. [CrossRef] [PubMed]
23. Pang, X.; Sellaoui, L.; Franco, D.; Dotto, G.L.; Georgin, J.; Bajahzar, A.; Belmabrouk, H.; Lamine, A.B.; Bonilla-Petriciolet, A.; Li, Z. Adsorption of crystal violet on biomass from pecan nutshell, para chestnut husk, araucaria bark and palm cactus: Experimental study and theoretical modelling via monolayer and double layer statistical physics models. *Chem. Eng. J.* **2019**, *378*, 122101. [CrossRef]
24. Zue, H.; Gao, X.; Sliem, M.; Mobarak, M.; Dong, R.; Wang, X.; Fu, K.; Li, Q.; Li, Z. Efficient adsorption of anionic azo dyes on porous heterostuctured MXene/biomass activated carbon composites: Experiments, characterization, and theoretical analysis via advanced statistical physis models. *Chem. Eng. J.* **2023**, *451*, 138735.
25. Tong, D.; Zhuang, J.; Lee, J.; Buchanan, J.; Chen, X. Concurrent transport and removal of nitrate, phosphate and pesticides in low-cost metal and carbon-based materials. *Chemosphere* **2019**, *230*, 84–91. [CrossRef]
26. Adesemuyi, M.F.; Adebayo, M.A.; Akinola, A.O.; Olasehinde, E.F.; Adewole, K.A.; Lajife, L. Preparation and characterisation of biochars from elephant grass and their utilisation for aqueous nitrate removal: Effect of pyrolysis temperature. *J. Environ. Chem. Eng.* **2020**, *8*, 104507. [CrossRef]
27. Banu, H.A.T.; Karthikeyan, P.; Meehakshi, S. Comparative studies on revival of nitrate and phosphate ions using quaternized corn husk and jackfruit peel. *Bioresour. Technol. Rep.* **2019**, *8*, 100331. [CrossRef]
28. Omo-Okoro, P.N.; Daso, A.P.; Okonkwo, J.O. A review of the application of agricultural wastes as precursor materials for the adsorption of per and plyfluoroalkyl substances: A focus on current approaches and methodologies. *Environ. Technol. Innov.* **2018**, *9*, 100–114. [CrossRef]
29. Wang, J.; Chen, C. Biosorbents for heavy metals removal and their future. *Biotechnol. Adv.* **2009**, *27*, 195–226. [CrossRef]
30. Zhang, M.; Song, G.; Gelardi, D.L.; Huang, L.; Khan, E.; Masek, O.; Parikh, S.J.; Ok, Y.S. Evaluating biochar and its modifications for the removal of ammonium, nitrate, and phosphate in water. *Water Res.* **2020**, *186*, 116303. [CrossRef]
31. Zolgharnein, J.; Asanjarani, N.; Shariatmanesh, T. Taguchi L_{16} orthogonal array optimization for Cd(II) removal using *Carpinus betulus* tree leaves. Adsorption characterization. *Inter. Biodeter. Biodegrad.* **2013**, *85*, 66–77. [CrossRef]
32. Rahul, D.; Pretesh, J. Application of Taguchi-based design of experiments for industrial chemical processes, statistical approaches with emphasis on design of experiments applied to chemical processes. *Valter Silva IntechOpen* **2018**, *69501*, 139.
33. Fernández-López, J.A.; Angosto, J.M.; Roca, M.J.; Doval Miñarro, M. Taguchi design-based enhancement of heavy metals bioremoval by agroindustrial waste biomass from artichoke. *Sci. Total Environ.* **2018**, *24*, 11154–11161. [CrossRef] [PubMed]

34. Yen, H.Y.; Lin, C.P. Adsorption of Cd(II) from wastewater using spent coffee grounds by Taguchi optimization. *Desalin. Wat. Treat.* **2016**, *24*, 11154–11161. [CrossRef]
35. Varala, S.; Kumari, A.; Dharanija, B.; Bhargava, S.K.; Parthasarathy, R.; Satyavathi, B. Removal of thorium (IV) from aqueous solutions by deoiled karanja seed cake: Optimization using Taguchi method, equilibrium, kinetic and thermodynamic studies. *J. Environ. Chem.* **2016**, *4*, 405–417. [CrossRef]
36. Pundir, R.; Chary, C.H.V.C.; Dastidar, M.G. Application of Taguchi method for optimizing the process parameters for the removal of copper and nickel by growing *Aspergillus* sp. *Water Res. Ind.* **2018**, *20*, 83–92. [CrossRef]
37. Wu, Y.; Fan, Y.; Zhang, M.; Ming, Z.; Yang, S.; Arkin, A. Functionalized agricultural biomass as a low-cost adsorbent: Utilization of rice straw incorporated with amine groups for the adsorption of Cr(VI) and Ni(II) from single and binary systems. *Biochem. Eng. J.* **2016**, *105*, 27–35. [CrossRef]
38. Hsieh, K.L.; Tong, L.I.; Chiu, H.P.; Yeh, H.Y. Optimization of a multi-response problem in Taguchi's dynamic system. *Comput. Ind. Eng.* **2005**, *4*, 556–571. [CrossRef]
39. Guo, X.; Wang, J. Comparison of linearization methods for modelling the Langmuir adsorption isotherm. *J. Mol. Liq.* **2019**, *296*, 111850. [CrossRef]
40. Srivastava, V.C.; Mall, I.D.; Mishra, I.M. Multicomponent adsorption study of metal ions onto bagasse fly ash using Taguchi´s design of experimental methodology. *Ind. Eng. Chem. Res.* **2007**, *46*, 5697–5706. [CrossRef]
41. Kumar, P.; Barrett, D.M.; Delwiche, M.J.; Stroeve, P. Methods for pretreatment of lignocellulosic biomass for efficient hydrolysis and biofuel production. *Ind. Eng. Chem. Res.* **2009**, *48*, 3713–3729. [CrossRef]
42. Boota, R.; Bhatti, H.N.; Hanif, M.A. Removal of Cu(II) and Zn(II) using lignocellulosic fiber derived from *Citrus reticulata* (kinnow) waste biomass. *Sep. Sci. Technol.* **2009**, *44*, 4000–4022. [CrossRef]
43. Ali, D.; Agarwal, R.; Hanifa, M.; Rawat, P.; Paswan, R.; Rai, D.; Tyagi, I.; Naik, S.; Pippal, A. Thermo-physical properties and microstructural behaviour of biochar-incorporated cementitious material. *J. Build. Eng.* **2023**, *64*, 105695. [CrossRef]
44. Aman, A.M.N.; Selvarajoo, A.; Lau, T.L.; Chen, W. Optimization via response surface methodology of palm kernel shell biochar for supplementary cementitious replacement. *Chemophere* **2023**, *313*, 137477. [CrossRef] [PubMed]
45. Fernández-López, J.A.; Doval Miñarro, M.; Angosto, J.M.; Fernández-Lledó, J. Adsoptive and surface characterization of Mediterranean agrifood processing wastes: Prospection for pesticide removal. *Agronomy* **2021**, *11*, 561. [CrossRef]
46. Parikh, J.; Channiwala, S.A.; Ghosal, G.K.A. A correlation for calculating elemental composition from proximate analysis of biomass materials. *Fuel* **2007**, *86*, 1710–1719. [CrossRef]
47. Barka, N.; Ouzaouit, K.; Abdennouri, M.; El Makhfouk, M. Dried prickly pear cactus (*Opuntia ficus indica*) cladodes as a low-cost and eco-friendly biosorbent for dyes removal from aqueous solutions. *J. Taiwan Int. Chem. Eng.* **2013**, *44*, 52–60. [CrossRef]
48. Nouri, H.; Abdedayem, A.; Hamidi, I.; Najjar, S.; Ouederni, A. Biosorption of lead heavy metal of prckly pear cactus biomaterial; kinetic, thermodynamic and regeneration studies. *Cellul. Chem. Technol.* **2021**, *55*, 932. [CrossRef]
49. Barrera, H.; Ureña-Núñez, F.; Bilyeu, B.; Barrera-Díaz, C. Removal of chromium and toxic ions present in mine drainage by Ectodermis of Opuntia. *J. Hazard. Mat.* **2006**, *136*, 846–853. [CrossRef]
50. Petrosyan, A.M.; Sukiasyan, R.P. Vibrational spectra of l-arginine nitrates. *J. Molec. Struct.* **2008**, *874*, 51–56. [CrossRef]
51. Guo, X.; Wang, J. A general kinetic model for adsorption: Theoretical analysis and modelling. *J. Molec. Liq.* **2019**, *288*, 111100. [CrossRef]
52. Wang, J.; Guo, X. Adsorption kinetic models: Physical meanings, applications, and solving methods. *J. Hazard. Mat.* **2020**, *390*, 122156. [CrossRef] [PubMed]
53. Zolfaghari, G.; Esmaili-Sari, A.; Anbia, M.; Younesi, H.; Amirmahmoodi, S.; Ghafari-Nazari, A. Taguchi optimization approach for Pb(II) and Hg(II) removal from aqueous solutions using modified mesoporous carbon. *J. Hazard. Mat.* **2011**, *192*, 1046–1055. [CrossRef]
54. Fotsing, P.N.; Bouazizi, N.; Woumfo, E.D.; Mofaddel, N.; Le Derf, F.; Vieillard, J. Investigation of chromate and nitrate removal by adsoption at the surface on an amine-modified cocoa shell adsorbent. *J. Environ. Chem. Eng.* **2021**, *9*, 104618. [CrossRef]
55. Wang, J.; Guo, X. Rethinking of the intraparticle diffusion adsorption kinetics model: Interpretation, solving methods and applications. *Chemosphere* **2022**, *309*, 136732. [CrossRef]
56. Dovi, E.; Aryee, A.; Li, J.; Li, Z.; Qu, L.; Han, R. Amine-grafted walnut shell for efficient removal of phosphate and nitrate. *Environ. Sci. Pollut. Res.* **2021**, *29*, 20976–20995. [CrossRef]
57. Foo, K.Y.; Hameed, B.H. Insights into the modelling of adsorption isotherm systems. *Chem. Eng. J.* **2010**, *156*, 2–10. [CrossRef]
58. Weber, T.W.; Chakravorti, R.K. Pore and solid diffusion models for fixed-bed adsorbers. *AIChE J.* **1974**, *20*, 228–238. [CrossRef]
59. Karnitz, O., Jr.; Gurgel, L.V.A.; De Melo, J.C.P.; Botaro, V.R.; Melo, T.M.S.; de Freitas Gil, R.P.; Gil, L.F. Adsorption of heavy metal ion from aqueous single metal solution by chemically modified sugarcane bagasse. *Bioresour. Technol.* **2007**, *98*, 1291–1297. [CrossRef]
60. Bulut, E.; Ozacar, M.; Sengil, A. Adsorption of malachite green onto bentonite: Equilibrium and kinetic studies and process design. *Microp. Mesop. Mat.* **2008**, *115*, 234–246. [CrossRef]
61. Obon, J.M.; Angosto, J.M.; González-Soto, F.; Ascua, A.; Fernández-López, J.A. prototyping a spinning adsorber submerged filter for continuous removal of wastewater contaminants. *J. Water Proc. Eng.* **2022**, *45*, 102515. [CrossRef]
62. Yang, L.; Yang, M.; Xu, P.; Zhao, X.; Bai, H.; Li, H. Characteristics of nitrate removal from aqueous solution by modified steel slag. *Water* **2017**, *9*, 757. [CrossRef]

63. Fotsing, P.N.; Woumfo, E.D.; Mezghich, S.; Mignot, M.; Moffadel, N.; Le Derf, F.; Viellard, J. Surface modification of biomaterials bases on cocoa shell with improve nitrate and Cr (VI) remova. *RSC Adv.* **2020**, *10*, 20009–20019. [CrossRef]
64. Ren, Z.; Xu, X.; Wang, X.; Gao, B.; Yue, Q.; Song, W.; Zhang, L.; Wang, H. FITIR, Raman and XPS analysis during phosphate, nitrate and Cr (VI) removal by amine cross-linking biosorbent. *J. Coll. Sci.* **2016**, *468*, 313–323.
65. Quiao, H.; Mei, L.; Chen, G.; Liu, H.; Peng, C.; Ke, F.; Hour, R.; Wan, X.; Cai, H. Adsorption of nitrate and phosphate aqueous solution using amne cross-linked tea wastes. *Appl. Surf. Sci.* **2019**, *483*, 114–122. [CrossRef]
66. Keränen, A.; Leiviskä, T.; Hormi, O.; Tanskanen, J. Removal of nitrate by modified pine sawdust: Effects of temperature and co-existing anions. *J. Environ. Manag.* **2015**, *147*, 46–54. [CrossRef]